AIAA JOURNAL
Vol. 32, No. 12, December 1994

Critical Load Analysis of Undamped Nonconservative Systems Using Bieigenvalue Curves

Shyh-Rong Kuo*
National Taiwan Ocean University, Keelung, Taiwan 20224, Republic of China
and
Yeong-Bin Yang†
National Taiwan University, Taipei, Taiwan 10617, Republic of China

To study the instability of an undamped nonconservative system using the finite element method, an asymmetric load matrix has to be included to account for the path-dependent nature of the applied loads, in addition to the mass matrix, elastic stiffness matrix, and geometric stiffness matrix. Before the critical loads can be determined for a structure, one basic problem in research of this sort has been the construction of load-frequency relationships from the eigenvalue equations. Traditionally, this requires solution of complex eigenvalues from the characteristic equations at many load levels, which in practice is very time consuming. In this paper, an efficient approach based on a fourth-order hyperbolic curve will be proposed for predicting the critical loads. This curve, also known as the bieigenvalue curve, can be uniquely determined, once the first and second derivatives of the frequency with respect to the load parameter have been calculated for the structure under a preset load level, based on the eigensolutions for the first few or all modes of vibration. Effectiveness and accuracy of the procedure based on the bieigenvalue curve is demonstrated in the numerical study.

Introduction

A NONCONSERVATIVE system is characterized by the fact that the work done by the applied loads is path dependent. Failure of structures under the action of nonconservative loads has not been uncommon in the literature. One famous example has been the collapse of Tacoma Narrows Bridge in 1940 under the action of wind gusts, which, known as one type of follower forces, are nonconservative in nature. Unlike structures under the action of conservative loads, say, loads of the gravity type, a structure acted upon by nonconservative loads may become unstable in the form of flutter (or dynamic) instability, in addition to divergence (or static) instability. Whether a nonconservative structure may fail by flutter or divergence instability depends on the geometry of the structure and the type of boundary conditions imposed. To analyze the instability of nonconservative systems, dynamic approaches that consider the effect of inertial forces should be adopted.

The instability of nonconservative structures have been treated by many previous researchers.[1-3] In earlier studies, various methods such as the Galerkin method, Ritz method, and Hamilton's principle have been employed. However, these methods share one feature in common in that their applications are restricted mostly to simple problems, such as cantilevers or simply supported beams. To analyze the instability of more complicated structures, general numerical methods such as the finite element method have to be adopted.[4-6] With the finite element method, it is possible to formulate the characteristic equations for the structure considered, in which an asymmetric load stiffness matrix has to be introduced to account for the nonconservative nature of the applied loads. Traditional approaches aimed at establishing the load-frequency relationship of the dynamic problem require multiple solutions of complex eigenvalues from the characteristic equations, which are time consuming in practice. To improve the efficiency of solution, a bisection scheme based on the eigenvalue sensitivity has been proposed in Ref. 7. However, such a scheme is not always reliable, since it may fail for problems with instability of the divergence type.

In this paper, a fourth-order hyperbolic curve will be proposed for approximating the load-frequency relations that are typical for undamped nonconservative systems. With this curve, the critical loads can be predicted in a computationally efficient manner, regardless of the types of instability. One merit with the present approach is that the determination of the bieigenvalue curve does not require full eigenvalue solutions of the complex problem. Therefore, methods that are suitable for extracting the first few eigensolutions, such as the one presented in Ref. 8, can be employed to enhance further the efficiency of the present scheme.

Received Oct. 22, 1993; revision received July 6, 1994; accepted for publication July 6, 1994.

*Associate Professor, Department of Harbor and River Engineering.
†Professor, Department of Civil Engineering.

Load Stiffness Matrix

Consider the frame element of 12 degrees of freedom shown in Fig. 1. To describe the behavior of a follower force, say, acting at node A of the element, two sets of coordinates will be needed. One is the stationary coordinates xyz, and the other is the moving coordinates $\alpha\beta\gamma$ (Fig. 2). In the following, the prebuckling configuration of a structure will be identified as the C_1 configuration and the buckling configuration as the C_2 configuration. According to Fig. 2, the follower force $(F_\alpha, F_\beta, F_\gamma)$ has the following components at C_1:

$$\{{}^1\boldsymbol{F}\}^T = \begin{Bmatrix} {}^1F_x & {}^1F_y & {}^1F_z \end{Bmatrix} \tag{1}$$

with reference to the xyz axes.

Let us use $\{\boldsymbol{u}\}$ to denote the displacements of node A of the element during the buckling process from C_1 to C_2, i.e.,

$$\{\boldsymbol{u}\}^T = \{\{\boldsymbol{d}\}^T \quad \{\boldsymbol{\theta}\}^T\} \tag{2}$$

where

$$\{\boldsymbol{d}\}^T = \{u \quad v \quad w\} \tag{3a}$$

$$\{\boldsymbol{\theta}\}^T = \{\theta_x \quad \theta_y \quad \theta_z\} \tag{3b}$$

For the cases where the rotations $\{\boldsymbol{\theta}\}$ are small, the transformation matrix $[\boldsymbol{T}]$ that relates the axes $\alpha\beta\gamma$ from the C_1 to the C_2 state is simply

$$[\boldsymbol{T}] = \begin{bmatrix} 1 & \theta_z & -\theta_y \\ -\theta_z & 1 & \theta_x \\ \theta_y & -\theta_x & 1 \end{bmatrix} \tag{4}$$

Consequently, the follower force $(F_\alpha, F_\beta, F_\gamma)$ at the C_2 configuration can be referred to the axes at C_1 as

$$\{{}^2\boldsymbol{F}\} = [\boldsymbol{T}]\{{}^1\boldsymbol{F}\} = \{{}^1\boldsymbol{F}\} + \{\Delta\boldsymbol{F}\} = \{{}^1\boldsymbol{F}\} + [\boldsymbol{k}_f]\{\boldsymbol{\theta}\} \tag{5}$$

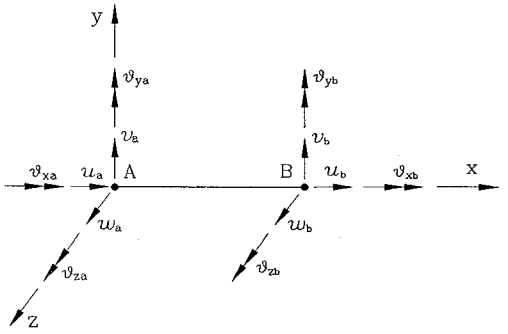

Fig. 1 Space frame element.

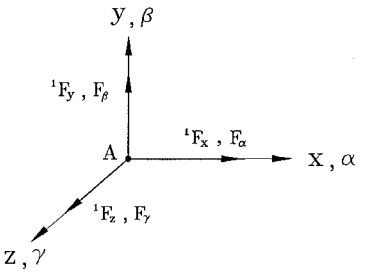

a)

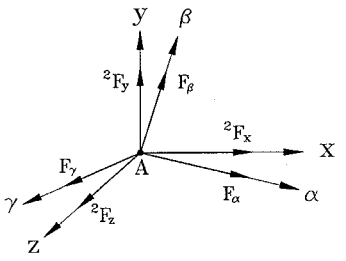

b)

Fig. 2 Follower forces: a) C_1 configuration and b) C_2 configuration.

where the matrix $[k_f]$ accounts for the path-dependent nature of the applied loads,

$$[k_f] = \begin{bmatrix} 0 & {}^1F_z & -{}^1F_y \\ -{}^1F_z & 0 & {}^1F_x \\ {}^1F_y & -{}^1F_x & 0 \end{bmatrix} \tag{6}$$

The last term in Eq. (5), i.e., $\{\Delta F\}$, represents the forces induced by the follower force undergoing rotations.

The virtual works done by the follower force at C_1 and C_2 are

$$^1\delta W = \{\delta d\}^T\{^1F\} \tag{7}$$

$$^2\delta W = \{\delta d\}^T\{^2F\} = \{\delta d\}^T\{^1F\} + \{\delta d\}^T[k_f]\{\theta\} \tag{8}$$

Subtracting Eq. (7) from Eq. (8) yields the virtual work done by the induced forces during the buckling process

$$\{\delta d\}^T[k_f]\{\theta\} = \{\delta u\}^T[k_l]\{u\} \tag{9}$$

where the displacement vector $\{u\}$ has been defined in Eq. (2) for node A of the element (Fig. 1) and the load stiffness matrix $[k_f]$ is

$$[k_l] = \begin{bmatrix} [0] & [k_f] \\ [0] & [0] \end{bmatrix} \tag{10}$$

which, as can be seen, is asymmetric. Though the derivation has been made here only for node A, it can be easily extended to treat node B of the element.

Linearized Theory of Stability

With the load stiffness matrix $[k_l]$ already derived, and the elastic stiffness matrix $[k_e]$, geometric stiffness matrix $[k_g]$, and mass matrix $[m]$ available elsewhere,[9–11] the equation of motion can be written for each element. This equation can then be assembled, by looping over all of the elements of a structure, to yield the equation of motion for the structure in incremental form as

$$[M]\{\ddot{U}\} + ([K_e] + [K_g] - [K_l])\{U\} = \{^2P\} - \{^1P\} \tag{11}$$

where quantities associated with the structure have been expressed in upper case letters, and $\{^1P\}$ and $\{^2P\}$ denote the applied loads acting on the structure at the C_1 and C_2 configurations, respectively. In particular, the vector $\{U\}$ denotes the buckling deformation of the structure from C_1 to C_2. For the cases where the prebuckling deformations of the structure are negligibly small, both the $[M]$ and $[K_e]$ matrices can be regarded as constant, and the $[K_g]$ and $[K_l]$ matrices are proportional to the applied loads. Moreover, it is assumed that the applied loads acting on the structure remain constant as buckling occurs, i.e.,

$$\{^2P\} = \{^1P\} = \lambda\{\bar{P}\} = \{P\} \tag{12}$$

where $\{\bar{P}\}$ denotes the reference loads and λ the associated load parameter. In accordance,

$$[M]\{\ddot{U}\} + ([K_e] + \lambda[\bar{K}_g] - \lambda[\bar{K}_l])\{U\} = \{0\} \tag{13}$$

where $[\bar{K}_g]$ and $[\bar{K}_l]$ denote the matrices evaluated for the structure under the action of the reference loads $\{\bar{P}\}$ prior to buckling.

By letting $\{U\} = \{\bar{U}\}e^{i\omega t}$, where ω denotes the frequency of vibration of the structure under the action of applied loads, the preceding equation reduces to

$$\left(-\omega^2[M] + [K_e] + \lambda[\bar{K}_g] - \lambda[\bar{K}_l]\right)\{\bar{U}\} = \{0\} \tag{14}$$

where both λ and ω^2 are eigenvalues and $\{\bar{U}\}$ denotes the associated eigenvector. Whether a structure will remain stable or not under the action of the applied loads $\{\bar{P}\}$ can be observed from the properties of the frequency of vibration ω. For instance, by letting $\omega = a + ib$, one can write

$$\{U\} = \{\bar{U}\}e^{iat} \cdot e^{-bt} \tag{15}$$

Evidently, as the imaginary part of ω, i.e., the variable b, turns out to be negative, the displacements $\{U\}$ of the structure will grow without bound. In this case, the structure is regarded as unstable.

Two types of instability can be identified for structures subjected to nonconservative loadings. One is the so-called static instability or divergence, which is characterized by the occurrence of negative ω^2 when the load parameter λ exceeds the critical value of λ_{cr} (Fig. 3a). To solve for λ_{cr}, one may set ω^2 in Eq. (14) equal to zero, i.e.,

$$([K_e] + \lambda_{cr}[\bar{K}_g] - \lambda_{cr}[\bar{K}_l])\{\bar{U}\} = \{0\} \tag{16}$$

For this particular case, the eigenvalue λ_{cr} can be determined by a single call to any eigenvalue solver that is capable of dealing with asymmetric matrices or complex eigenvalues.

On the other hand, the dynamic instability or flutter of a structure is typified by the occurrence of complex ω^2 once the load parameter λ exceeds the critical value λ_{cr} (Fig. 3b). For the special case of $\lambda = \lambda_{cr}$, two identical roots ω^2 will occur. To solve for the critical value λ_{cr}, one conventional approach is to divide the loadings $\{P\}$ into a number of increments, as shown in Fig. 4a, and then solve for the eigenvalues ω^2 corresponding to each load level. By plotting the load parameters λ against the frequencies ω^2 obtained for all load levels, the critical value λ_{cr} can be determined. Here, it should be noted that to obtain solutions of sufficient accuracy, much smaller load steps (say, determined by the bisection scheme) should be used when approaching the critical load λ_{cr} (see Fig. 4a). Although the amount of computation involved can be reduced by seeking only for the first few modes, the requirement of multiple calls to the complex eigenvalue solver remains a serious bottleneck. In the following, an approximate but very efficient approach will be proposed for solving the critical loads.

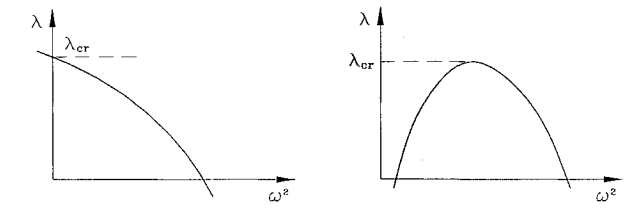

Fig. 3 Types of instability: a) divergence and b) flutter.

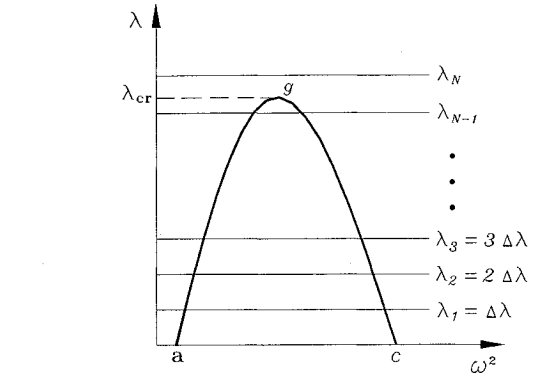

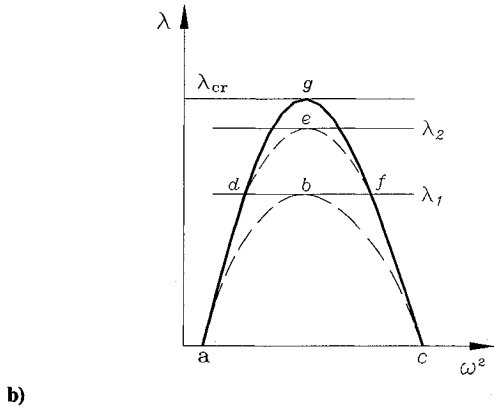

Fig. 4 Methods of solution: a) conventional and b) present.

Derivatives for Bieigenvalue Problems

Let α_i^2 and $\{v_i\}$ denote the ith mode of eigenvalue and eigenvector of a J dimensional subset of an N-degree-of-freedom system that is free of any applied loads, i.e.,

$$\left(-\alpha_i^2[M]+[K_e]\right)\{v_i\}=\{0\} \tag{17}$$

where $i = 1, 2, \ldots, J$ and $J \leq N$. Moreover, let $[V]$ denote the modal matrix comprising of only the first J eigenvectors, i.e., $[V] = [\{v_1\}, \ldots, \{v_J\}]$. The following properties of orthogonality are known to be valid:

$$[V]^T[M][V]=[I] \tag{18}$$

$$[V]^T[K_e][V]=[\Lambda]=\begin{bmatrix}\ddots & & 0\\ & \alpha_i^2 & \\ 0 & & \ddots\end{bmatrix} \tag{19}$$

With these properties, Eq. (14) can be converted to the following:

$$(-\omega_i^2[I]+[\Lambda]+\lambda[A])\{\phi_i\}=\{0\} \tag{20}$$

$$\{\psi_i\}^T\left(-\omega_i^2[I]+[\Lambda]+\lambda[A]\right)=\{0\}^T \tag{21}$$

where $\{\phi_i\}$ and $\{\psi_i\}$ are the right and left eigenvectors of the ith mode, and

$$[A]=[V]^T([\bar{K}_g]-[\bar{K}_l])[V] \tag{22}$$

By letting $[\Phi] = [\{\phi_1\}, \ldots, \{\phi_J\}]$ and $[\Psi] = [\{\psi_1\}, \ldots, \{\psi_J\}]$, it can be shown that

$$[\Psi]^T[\Phi]=[I] \tag{23}$$

Differentiating Eq. (20) with respect to λ yields

$$(-\mathrm{d}\omega_i^2/\mathrm{d}\lambda[I]+[A])\{\phi_i\}+[B_i]\frac{\mathrm{d}}{\mathrm{d}\lambda}\{\phi_i\}=\{0\} \tag{24}$$

where

$$[B_i]=-\omega_i^2[I]+[\Lambda]+\lambda[A]=[\Phi][D_i][\Psi]^T \tag{25}$$

with the diagonal matrix $[D_i]$ defined as

$$[D_i]=\begin{bmatrix}\omega_1^2-\omega_i^2 & & 0\\ & \ddots & \\ 0 & & \omega_J^2-\omega_i^2\end{bmatrix} \tag{26}$$

Multiplying Eq. (24) by $\{\psi_i\}^T$ and using Eq. (21), one can show that the following relation is valid:

$$\frac{\mathrm{d}\omega_i^2}{\mathrm{d}\lambda}=\{\psi_i\}^T[A]\{\phi_i\}=a_i^* \tag{27}$$

Meanwhile, multiplying Eq. (24) by $[\Psi]^T$ and utilizing the relations in Eqs. (23), (25) and (27), the following can be derived:

$$[D_i][\Psi]^T\frac{\mathrm{d}}{\mathrm{d}\lambda}\{\phi_i\}=[\Psi]^T(a_i^*[I]-[A])\{\phi_i\} \tag{28}$$

As can be seen from Eq. (26), the $[D_i]$ matrix is singular because its ith diagonal element vanishes. Correspondingly, it can be observed that the ith component on the right-hand side of Eq. (28) also equals zero. To solve this equation, one may define a matrix called $[S_i]$ that contains only one nonzero entry S_i in its ith diagonal element. With the aid of this matrix, Eq. (28) can be solved as

$$\frac{\mathrm{d}}{\mathrm{d}\lambda}\{\phi_i\}=[\Phi]([D_i]+[S_i])^{-1}[\Psi]^T(a_i^*[I]-[A])\{\phi_i\} \tag{29}$$

By the relations $[\Phi] = [\Psi]^{-T}$, $[\Psi]^T = [\Phi]^{-1}$, and Eq. (25),

$$\frac{\mathrm{d}}{\mathrm{d}\lambda}\{\phi_i\}=\left([B_i]+[\Phi][S_i][\Psi]^T\right)^{-1}(a_i^*[I]-[A])\{\phi_i\} \tag{30}$$

where it is noted that $[\Phi][S_i][\Psi]^T = S_i\{\phi_i\}\{\psi_i\}^T$. As the first derivatives of ω^2 and $\{\phi_i\}$ with respect to λ are made available, some further calculations can be performed.

First, by differentiating Eq. (24) with respect to λ, one obtains

$$-\mathrm{d}^2\omega_i^2/\mathrm{d}\lambda^2\{\phi_i\}+2(-\mathrm{d}\omega_i^2/\mathrm{d}\lambda[I]+[A])\frac{\mathrm{d}}{\mathrm{d}\lambda}\{\phi_i\}$$

$$+[B_i]\frac{\mathrm{d}^2}{\mathrm{d}\lambda^2}\{\phi_i\}=\{0\} \tag{31}$$

Then, by multiplying this equation by the left eigenvector $\{\psi_i\}^T$, along with the use of Eq. (21), one can show that

$$\mathrm{d}^2\omega_i^2/\mathrm{d}\lambda^2=-2\{\psi_i\}^T\left(a_i^*[I]-[A]\right)\frac{\mathrm{d}}{\mathrm{d}\lambda}\{\phi_i\} \tag{32}$$

This is exactly the second derivative of ω^2 with respect to λ, if use is made of the expression for $\mathrm{d}\{\phi_i\}/\mathrm{d}\lambda$ in Eq. (30).

Solutions Based on Approximate Bieigenvalue Curves

In the preceding section, one has illustrated how the first and second derivatives of the frequency of vibration with respect to the load parameter can be calculated for a particular problem. Such information is useful in determining the fourth-order hyperbolic curve proposed for simulating the load-frequency relation of undamped nonconservative structures, as follows:

$$(\omega^2 - a_1 - b_1\lambda)(\omega^2 - a_2 - b_2\lambda) + \lambda^2(e_1\omega^2 + e_2) = 0 \quad (33)$$

Here, one realizes that a single solution of the eigenvalue problem in Eq. (14) will yield two frequencies of vibration. To determine the six coefficients for the approximate bieigenvalue curve proposed in Eq. (33), six conditions need be specified. All such conditions can be obtained from the two frequencies of vibration solved and their corresponding first and second derivatives calculated. In particular, one may regard the coefficients a_1, b_1 and a_2, b_2 in Eq. (33) as the frequency of vibration and its first derivative for the two modes of vibration solved.

If the coefficient e_1 is omitted, then Eq. (33) reduces to a hyperbolic curve that can simulate exactly the bieigenvalue relation of a two-degree-of-freedom system. The coefficient e_2 can be approximately regarded as a representation of the interaction effect of induced forces on the two eigenvalues. The coefficient e_1, however, can be interpreted as the influence of other modes on the two modes of vibration in connection with the induced force components. It should be noted that all of the coefficients in Eq. (33) will always appear as real numbers, regardless of whether the estimated load λ_{cr} is greater or smaller than the true value.

The following is the procedure proposed for calculating the critical load λ_{cr} of structures based on the approximate bieigenvalue curve.

1) Solve the eigenvalue problem with symmetric matrices in Eq. (17) for the frequencies for the structure in free vibration, and select the two adjacent modes that have the smallest difference in the frequency of vibration, which have been identified as points a and c in Fig. 4b.

2) Use Eqs. (27), (30), and (32) to calculate the first and second derivatives of ω^2 with respect to λ. Substitute these values into Eq. (33) to obtain the first approximate bieigenvalue curve, which has been identified as curve abc in Fig. 4b.

3) Calculate the approximate critical load λ_1 from Eq. (33) (see Fig. 4b).

4) Solve the asymmetric eigenvalue problem in Eqs. (20) and (21) for ω^2 with λ set equal to λ_1. This result corresponds to points d and f in Fig. 4b.

5) Again, use Eqs. (27), (30), and (32) to calculate $d\omega^2/d\lambda$ and $(d^2\omega^2)/(d\lambda^2)$. Substitute these values into Eq. (33) to obtain the improved curve, which has been denoted as curve def in Fig. 4b.

6) Calculate the improved critical load λ_2 from curve def.

7) Repeat steps 4–6 until the difference between the critical loads λ_{cr} obtained from two consecutive runs of analysis is smaller than a preset tolerance value.

Experience has told us that for most nonconservative problems, only very few number of iterations, normally less than three, are required to obtain solutions that are of sufficient accuracy.

Numerical Examples

The efficiency and reliability of the procedure proposed in the preceding section based on the approximate bieigenvalue curves will be numerically evaluated in this section through the study of three examples.

Beam Subjected to Transverse Follower Load

As shown in Fig. 5, a beam with a length of $L = 270$ cm is subjected to a shear load P of the follower type at end B. It is restrained against translations along three axes and rotation about the x axis at end A and against rotations about the y and z axes at end B. The material properties adopted herein are: Young's modulus $E = 21\times10^5$ kg/cm^2 and shear modulus $G = 7.8\times10^5$ kg/cm^2. The beam is modeled by 10 elements of equal length. To investigate the effect of flutter instability, two types of cross sections are assumed for the beam. The following are the data for section 1: depth $b = 15.36$ cm, width $t = 0.75$ cm, area $A = 11.52$ cm^2, moment of inertia $I_y = 0.54$ cm^4, torsional constant $J = 2.16$ cm^4, radius of gyration squared $r^2 = 19.71$ cm^2, and specific weight $\gamma = 7.5 \times 10^{-3}$ kg/cm^3. With these sectional properties, the frequencies ω^2 solved from the free vibration analysis for the first three flexural modes are 14.75 s^{-2}, 1195 s^{-2}, and 9220 s^{-2}; and for the torsional mode it is 32,700 s^{-2}. Of interest to note is that if the applied load P is assumed to be of the conservative type, the beam will buckle at a value of 40.15 kg.

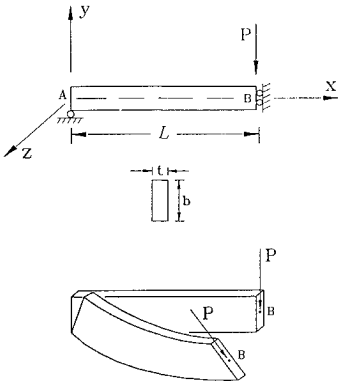

Fig. 5 Beam subjected to transverse follower load.

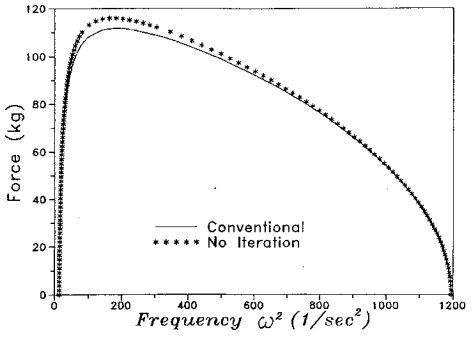

a)

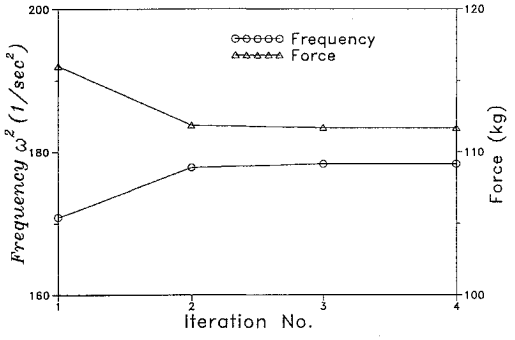

b)

Fig. 6 Beam with section 1: a) bieigenvalue curve and b) convergence rate.

For the present case, the dynamic instability of the structure is governed by the coalescence of the frequencies of vibration of the first two modes, since their difference appears to be the smallest compared with other pairs of higher modes. The solution obtained from the bieigenvalue curve has been plotted with no iteration in Fig. 6a, which deviates slightly from the solution obtained by the conventional approach. The accuracy of the present solution can be improved by performing the iteration procedure described in the preceding section. As can be seen from Fig. 6b, a very good solution can be obtained just within three cycles of iteration. For this particular case, the symmetric eigenvalue problem has been solved once and the asymmetric eigenvalue problem twice. The total CPU time consumed in such a process is 38.19 s using an 80486 personal computer.

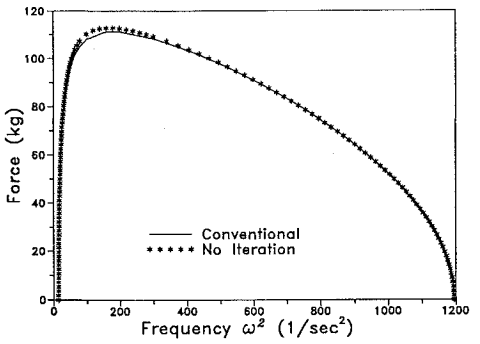

a)

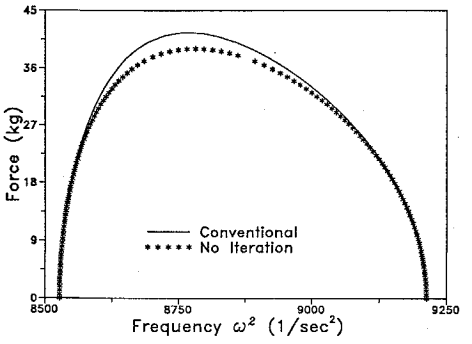

b)

Fig. 7 Bieigenvalue curve for beam with section 2: a) low-frequency range and b) high-frequency range.

The solution obtained by the conventional approach has also been plotted in Fig. 6a. With this method, it can be said that there is virtually no unique way for selecting the load increments and that the way by which the load increments are determined affects drastically the efficiency of computation. For this example, one has arbitrarily set the load increment to be $\Delta\lambda = 3$ kg and use the bisection scheme to subdivide the load increments whenever the critical load λ_{cr} is exceeded. This has resulted in the solution of the symmetric eigenvalue problem for one time and the asymmetric eigenvalue problem for 44 times. The total CPU time consumed is 686.57 s, which is about 18 times that of the present approach based on the bieigenvalue curve. Although margins exist for improving the efficiency of the conventional scheme, it can still be ascertained that the scheme based on the bieigenvalue curve remains a highly competitive one, if not a superior one, as far as the efficiency of computation is concerned.

In reality, whether the dynamic instability will be triggered by the lower or higher modes depends fully on the cross-sectional properties of the beam. For the purpose of investigation, one may assume that the beam is made of section 2 with the following properties: $b = 30$ cm, $t = 0.6$ cm, $A = 18$ cm^2, $I_y = 0.54$ cm^4, $J = 2.16$ cm^4, $r^2 = 75.03$ cm^2, and $\gamma = 4.8 \times 10^{-3}$ kg/cm^3. Since the mass per unit length and the flexural and torsional rigidities of the beam are identical to those for section 1, the frequencies of vibration for the flexural modes remain the same as those for the first case. However, the use of a larger radius of gyration r will result in the decrease of the frequency of vibration ω^2 for the torsional mode to a value of 8,530 s^{-2}.

The bieigenvalue curve established for the first two flexural modes has been plotted in Fig. 7a, and that for the third flexural mode and the torsional mode in Fig. 7b. As can be seen, the solutions predicted by the present approach appear to be in good agreement with those obtained conventionally, even though no iterations have been performed. Moreover, for this particular problem, the dynamic (flutter) instability of the structure will be triggered by the coalescence of the frequencies of vibration of the third and fourth modes, because of their relative closeness in magnitude in comparison with those of the lower modes. By comparing the solution for section 2 with that for section 1, it is concluded that the critical load of a nonconservative system can be increased through enlargement of the difference between the frequencies of vibration for the two closest modes.

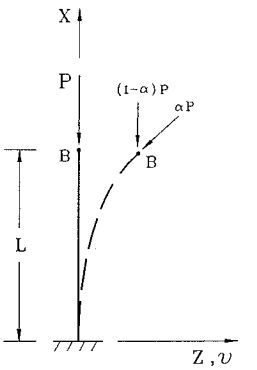

Fig. 8 Cantilever with axial load.

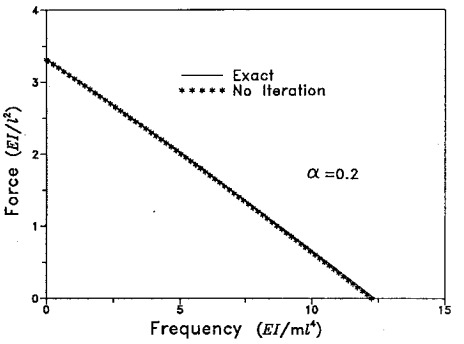

Fig. 9 Load-frequency curve, α = 0.2.

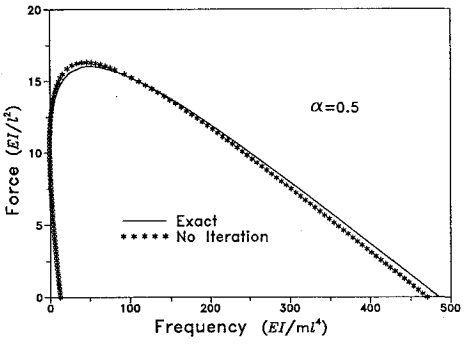

Fig. 10 Load-frequency curve, α = 0.5.

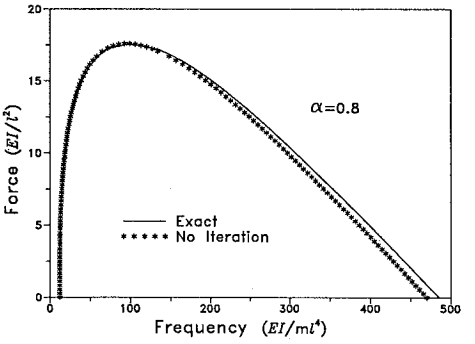

Fig. 11 Load-frequency curve, α = 0.8.

Cantilever with Nonconservative Axial Load

Figure 8 shows a cantilever subjected to an axial load P at the free end, of which αP indicates the nonconservative (follower) part of the load. Approximate and exact solutions for this problem are available in Refs. 12 and 13, respectively. For $\alpha < 0.5$, the stability of the cantilever is basically controlled by the conservative part of the load P, whereas for $\alpha > 0.5$, it is dominated by the nonconservative part.

In the numerical analysis, a 10-element mesh is used. The efficiency of the present approach was fully demonstrated in this example. For instance, one observes from Figs. 9–11 that the first

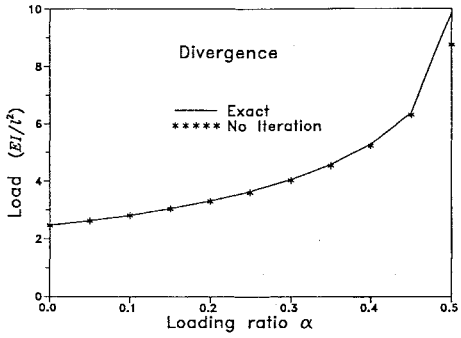

a)

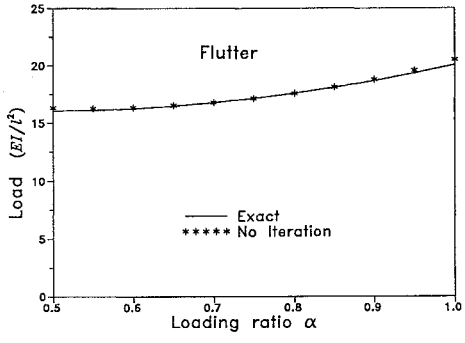

b)

Fig. 12 Critical loads: a) divergence and b) flutter.

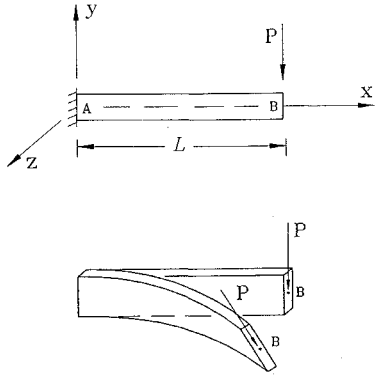

Fig. 13 Cantilever subjected to transverse follower load.

approximate solutions obtained by the present approach, based on a single solution of the symmetric eigenvalue problem, correlate very well with the theoretical ones, which renders any further iterations unnecessary. From Fig. 10, it can be observed that when α equals 0.5, the cantilever will become unstable both by divergence (as characterized by the condition $\omega^2 = 0$) and by flutter (as characterized by the existence of identical roots). The load P has been plotted against the parameter α for different ranges of α in Fig. 12.

Cantilever Subject to Transverse Follower Load

Consider the cantilever shown in Fig. 13, which is subjected to a transverse follower load P at the free end. For the first case, the cantilever is assumed to be made of section 2. With the cantilever divided into 10 elements in the free vibration analysis, the following frequencies ω^2 can be solved for the first three flexural modes: 29.92 s^{-2}, 1176 s^{-2}, and 8760 s^{-2}; and the following for the torsional mode: 8520 s^{-2}. As a side note, the buckling load for the cantilever is 76.09 kg, if assumed to be of the conservative type. The bieigenvalue curves calculated for the first two pairs of modes of vibration have been plotted in Figs. 14a and 14b. From these figures, the accuracy and effectiveness of the present procedure has been demonstrated to be excellent. Also evident from these figures is that the dynamic instability of the cantilever will be governed by the higher modes.

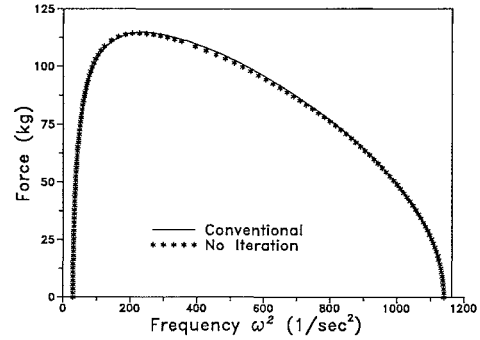

a)

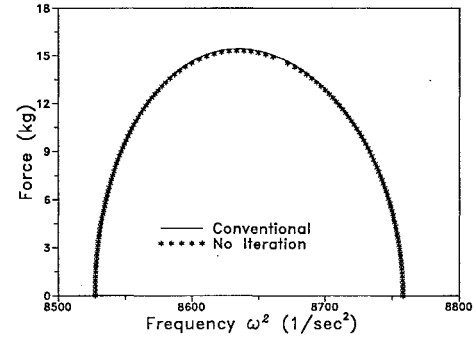

b)

Fig. 14 Bieigenvalue curve for cantilever with section 2: a) low-frequency range and b) high-frequency range.

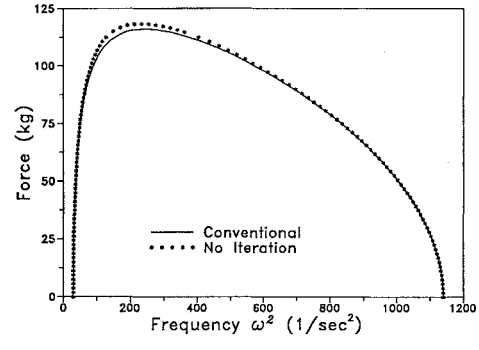

Fig. 15 Bieigenvalue curve for cantilever with section 1.

Such a situation can be reversed if section 1 is used for the cantilever. In this case, the frequency of vibration ω^2 for the torsional mode will be dramatically increased, reaching a value of 32,000 s^{-2}, and the dynamic instability will be dominated by the lower modes (Fig. 15).

Concluding Remarks

In a displacement-based finite element analysis, the nonconservative effects of the applied loads is represented by an asymmetric load matrix. The conventional approach for calculating the critical load of a nonconservative system requires multiple solutions of the bieigenvalue equations at different load levels, which in practice is extremely time consuming, due to involvement of the asymmetric load matrix. An approximate bieigenvalue curve is proposed in this paper for simulating the load-frequency relations of undamped nonconservative systems. Such a curve can be easily determined, once the first and second derivatives of the frequency with respect to the load parameter are calculated, based on the eigensolutions for the first few or all modes of vibration. In the numerical study, it has been demonstrated that the proposed method can be effectively used in the prediction of critical loads for undamped structures subjected to nonconservative loads, with no regard to the type of instability. Also illustrated is the fact that the critical load of a nonconservative system can be increased through enlargement of the difference between the frequencies of vibration for the two closest modes.

Acknowledgments

The research reported herein has been sponsored in part by the National Science Council of the Republic of China through Grant NSC80-0410-E002-18. This paper has been significantly revised from a paper entitled "Instability of Undamped Nonconservative Systems," which was presented at the SEIKEN-IASS Symposium on Nonlinear Analysis and Design for Shell and Spatial Structures in Tokyo, Japan, on Oct. 20–22, 1993.

References

[1]Bolotin, V. V., *Nonconservative Problems of the Theory of Elastic Stability*, Moscow, English translation, Pergamon, New York, 1963.

[2]Leipholz, H. H. E., *Stability Theory*, Academic, New York, 1970.

[3]Ziegler, H., *Principles of Structural Stability*, 2nd ed., Birkhäuser, Stuttgart, Germany, 1977.

[4]Barsoum, R. S., "Finite Element Method Applied to the Problem of Instability of a Nonconservative System," *International Journal for Numerical Methods in Engineering*, Vol. 3, 1971, pp. 63–87.

[5]Mote, C. D., "Nonconservative Stability by Finite Element Method," *Journal of Engineering Mechanics Division*, ASCE, Vol. 97, No. 2, 1971, pp. 645–656.

[6]Argyris, J. H., Straub, K., and Symeonidis, S., "Nonlinear Finite Element Analysis of Elastic Systems under Nonconservative Loading—Natural Formulation Part II. Dynamic Problem," *Computer Methods in Applied Mechanics and Engineering*, Vol. 28, 1981, pp. 241–258.

[7]Chen, L. W., and Ku, D. M., "Stability of Nonconservative Systems Using Eigenvalue Sensitivity," *Journal of Engineering Mechanics*, ASCE, Vol. 117, No. 5, 1991, pp. 974–985.

[8]Sorensen, D. C., "Implicit Application of Polynomial Filters in a k-step Arnoldi Method," *SIAM Journal on Matrix Analysis and Applications*, Vol. 13, No. 1, 1990, pp. 357–385.

[9]Yang, Y. B., and Kuo, S. R., *Theory and Analysis of Nonlinear Framed Structures*, Prentice-Hall, Singapore, 1994.

[10]Yang, Y. B., and Kuo, S. R., "Consistent Frame Buckling Analysis by Finite Element Method," *Journal of Structural Engineering*, ASCE, Vol. 117, No. 4, 1991, pp. 1053–1069.

[11]Paz, M., *Microcomputer-Aided Engineering Structural Dynamics*, Van Nostrand, New York, 1986.

[12]Huseyin, K., *Vibrations and Stability of Multiple Parameter Systems*, Sijthoff and Noordhoff, Alphen aan den Rijn, The Netherlands, 1978.

[13]Kuo, S. R., "Theory of Static and Dynamic Stability for Space Frames," Ph.D. Thesis, Dept. of Civil Engineering, National Taiwan Univ., Taipei, Taiwan, ROC, June 1991 (in Chinese).